

# SATELLITE IMAGE CO-REGISTRATION BASED ON HYBRID INVARIANT LOCAL FEATURES

<sup>1</sup>R. SWATHI,<sup>2</sup>DR. A. SREENIVAS

<sup>1</sup>Asst. Prof, Prasad V Potluri Siddhartha Institute of Technology, Department of Electronic and Electrical engineering, India

<sup>2</sup>Associate Professor, Gitam University, Department of Electronics and Communication Engg., India

E-mail: <sup>1</sup>sbm\_movaa@pvpsiddhartha.ac.in, <sup>2</sup>drallurisreenivas@gmail.com

## ABSTRACT

It is a challenging task to attain significant automatic registration between the two satellite images due to variation in illumination and resolution of the images, dissimilar perspectives and the local deformations within the image. These concerns are rectified by an automatic registration scheme depends on a hybrid invariant feature combination of both Speeded-Up Robust Features (SURF) and Binary Robust Invariant Scalable Keypoints (BRISK). In the registration procedure, this feature combination speeds up the feature extraction and matching. Here, it makes the matching point pairs distributed consistently in satellite images and also further enhance the accuracy of input image rectification. Experimental results proves that the proposed scheme is very superior in Image Registration (IR) than the existing methods.

**Keywords:** *Automatic registration, Binary Robust Invariant Scalable Keypoints, Coarse matching, Speeded-Up Robust Features.*

## 1. INTRODUCTION

Multi-sensor imaging system is the recent and rapid development field in sensing technology [1]. Multi-sensor image fusion works on detection and matching of satellite image features taken from different sensor view-points [2], [3], [4]. This fused images are used in various applications like remote sensing, web mapping, land cover classification, computer vision and medical image analysis [5]. There are two approaches available in Satellite Image Co-registration (SIC) such as Feature Based Method (FBM) and Intensity Based method (IBM). Here, the objective of the image fusion is to associate matching information from a multi-sensor image of the similar scene by using FBM [6]. Such fused images are more sufficient for further image processing tasks like object identification, regional variation detection and image segmentation [7].

Several FBM techniques have been established over the past few years for correct detection and extraction of objects or important features from satellite image. Totally four steps involved in FBM for IR; feature extraction, feature matching and geometric transform and re-sampling [8]. Features extracted from the satellite images might be global or local features. Image pattern of the local features is commonly represented by its edge, corner and

points. Here, the selection of feature extraction depends on descriptor and matching scheme. In the past IR, Scale Invariant Feature Transform (SIFT), SURF, Oriented Binary Robust Independent Elementary (ORB) feature descriptors are commonly implemented [9]. These features has few limitations like illumination change and strong rotation angle [10]. In order to overcome these difficulties a hybrid feature combination is employed in this research.

The objective of this research focus on improving the performance of IR using hybrid feature combination and transform. In SIC, instead of implementing individual feature descriptor, a combination of feature descriptors (SURF and BRISK) are employed to enhance the accuracy of registration.

The remaining portion of the paper is organized as follows. Section II describes background material and related work. In Section III, describes hybrid feature based SIC algorithm. Section IV illustrates the registration performance of our method on various types of satellite image pairs with comparisons to other approaches, followed by some concluding remarks in Section V.

## 2. LITERATURE REVIEW

E. G. Parmehr *et al.* [11] have presented a bin size selection method in order to improve the registration reliability. This proposed scheme specified the best uniform (or) best variable bin size for the Probability Density Function (PDF), which was determined by analysis the association between related values of the data and the implemented geometric transformation. As compared with Feature Based Registration (FBR), superior performance was attained for the Intensity Based Registration (IBR) of aerial images of LiDAR data. While implementing IBR, the intensity of the image should be very high that was considered as one of the major drawback.

Tahoun *et al.* [12] have projected the performance of seven most effective descriptors in a FBR procedure. These features helped to separate the detector from the descriptor, which depends on the position of detected features. The descriptors were represented based on their repeatability and inliers ratio. Compared to all descriptors, the Good Features to Track (GFFT) and Harris descriptors showed an improved performance in automatic satellite registration.

X. Ni *et al.* [13] have illustrated an automatic registration approach, which was established on contour and SIFT. The registration technique executed a pre-registration by utilizing a contour feature matching procedure. The following procedure definite the overlapping region between the reference and input image. Once the coarse sections were gained, it performed a fine registration process depends on SIFT detector and local adaptive matching approach. The test result proved that the proposed scheme was very effective in registration.

L. J. Yang *et al.* [14] have demonstrated a novel affine method for IR by applying invariant feature extraction. The proposed scheme adapted the Salient Image Disks (SIDs) extraction technique in order to localize the features accurately in SAR images. Comparative experiments exhibited that the proposed scheme performed much superior than the original SID method in localization accuracy and stability of feature points. SAR-IR demonstrated

that this method was less sensitive and showed comparable result in registration.

Y. Ye *et al.* [15] have presented a local descriptors for multi-spectral remote sensing IR. The proposed scheme contained two-phase procedures, such as pre-registration and fine registration. Though, the pre-registration was done by utilizing the Scale Restriction-SIFT (SR-SIFT) to remove the obvious translation, rotation, and scale differences between the reference and the sensed image. Additionally, the fine registration stage represented the evenly distributed interest points were first extracted from the pre-registered image by utilizing the harris corner detector. After that, they embedded the Local Self-Similarity (LSS) descriptor as a similarity metric in order to identify the tie points among the reference and pre-registered image. The proposed scheme was assessed with three pairs of remote sensing images from TM, ETM+, ASTER, Worldview, and Quick-bird sensors. This literature mainly concentrated on outliers' rejection than the inlier's development. The test outcome indicated that the proposed scheme can gain a reliable registration.

To overcome the above mentioned drawbacks, an effective hybrid method is implemented in SIC, which enhances the procedure acclimated in the proposed strategy.

### 3. PROPOSED METHODOLOGY

This section broadly describe the proposed approach for SIC. Here, the initial input satellite images are capture from different view-points, sensors, at altered times, for identifying and matching the features. Generally, three kinds of feature levels available in image processing such as low level features, descriptor level features, and high level features.

In co-registration, low level features are ineffective in nature as it is not significant towards removing the weak points. Likewise, the high level features are effective, but it shows more computational complexity. Here, the descriptor level features are preferred to perform SIC. The general architecture of the SIC is represented below in figure 1,

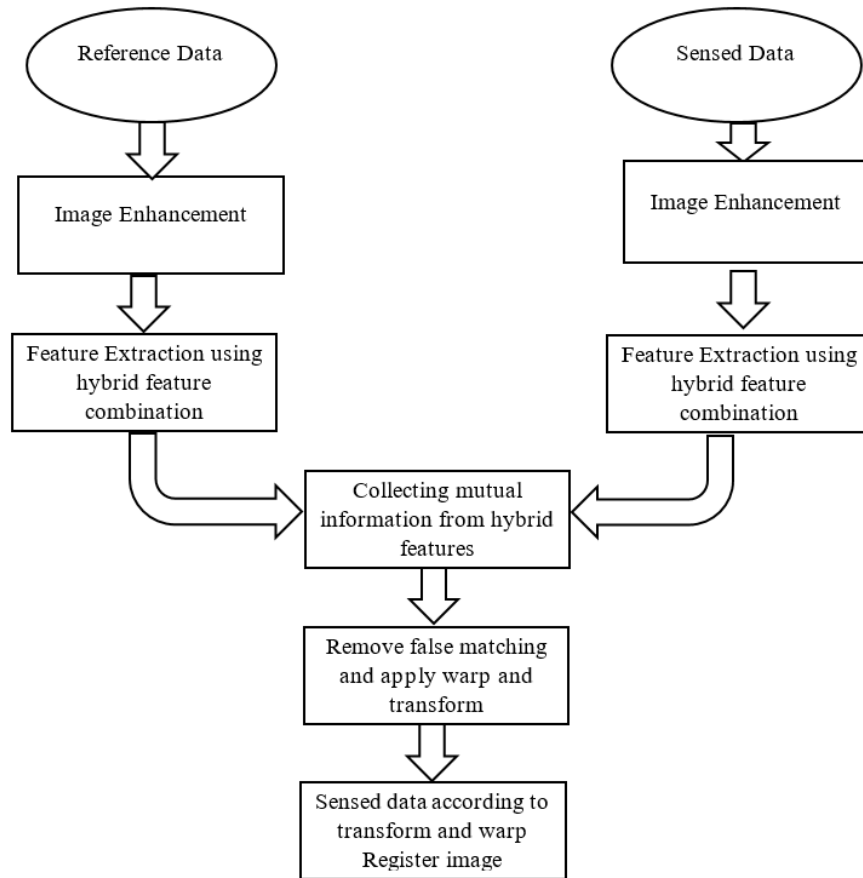


Figure 1: Procedure Followed In Image Registration

### 3.1 Hybrid Feature Combination in SIC

Through implementing hybrid feature selection (combination of SURF and BRISK), the global and local level features are extracted from the satellite image. The local features are analyzed by utilizing SURF, which is many times faster and more robust in processing several transformations in images than other descriptors and also it is very significant in integral image.

Similarly, the global features are separated by employing BRISK, which is implemented with a mechanism of orientation compensation in order to determine the orientation of keypoint and rotation. The following feature descriptors are explained and detailed below.

### 3.2 Speeded Up Robust Features (SURF)

The following section summarizes the SURF algorithm, it is a robust local feature descriptor that is widely utilized in computer vision applications. This algorithm contains three major steps such as Interest Point Localization (IPL), Integral Image Generation (IIG) and Interest Point Description (IPD). In SURF, the detection of key points depends on the scale space theory. In order to

determine the SURF features in an image  $I$ , this algorithm employs fast Hessian detector. Here, the Hessian Matrix (HM) is identified correspondingly to every pixel position of the image  $I$  and it is mathematically given by,

$$H(X, \sigma) = \begin{Bmatrix} C_{xx}(X, \sigma) & C_{xy}(X, \sigma) \\ C_{yx}(X, \sigma) & C_{yy}(X, \sigma) \end{Bmatrix} \quad (1)$$

Where,  $X$  is represented as the point of image,  $\sigma$  is mentioned as scale,

Normally,  $C_{xx}(X, \sigma)$  is denoted as the convolution of Gaussian second order derivative of image at the corresponding point with coordinates  $(x, y)$ . Gaussian second order derivative is represented as,

$$\frac{\partial^2}{\partial x^2} g(\sigma), \quad g(\sigma) = \frac{1}{2\pi\sigma^2} e^{-\frac{(x^2+y^2)}{2\sigma^2}} \quad (2)$$

Likewise, the second order Gaussian derivative for  $C_{yy}(X, \sigma)$  and  $C_{xy}(X, \sigma)$  are respectively given as follows,

$$\frac{\partial^2}{\partial y^2} g(\sigma) \text{ and } \frac{\partial^2}{\partial x \partial y} g(\sigma) \quad (3)$$

In SURF, a simple box filter is utilized as the approximation of convolution Gaussian second order derivative in smooth image, it makes the operation with less computational complexity. Here, the box filters are computed in constant time by utilizing integral images and this integral images are employed to achieve convolution of box filters  $B_{xx}$ ,  $B_{yy}$ , and  $B_{xy}$ . The approximate determinant of the HM is employed to identify the key-point, which is mentioned as follows,

$$Det[H(X, \sigma)] = B_{xx} B_{yy} - (0.912 B_{xy})^2 \quad (4)$$

Where, 0.912 is utilized to stable the HM determinant,

In order to attain scale invariance, SURF employs box filters on the image to examine and match interest points. Hence, the box filters of altered sizes construct the scale space, which is portioned into octaves. The approximate determinant of HM is determined at various scales and the non-maximum suppression in  $3 \times 3 \times 3$  neighborhood is implemented to identify the maxima. With the reference of the maximum values, the SURF key point's location and scale  $\sigma$  are obtained. An orientation is allocated to the obtained key-point by determining the Haar-Wavelet (HW) response within its neighborhood radius  $6s$  ( $s$  means sampling steps).

The next step involved in the SURF feature is extracting the descriptor at the key-point. The orientation direction is allocated to the center of key-point, a square size of  $20s$ . Respectively, the square size is partitioned into  $4 \times 4$  sub-regions, each sub-region is further classified into  $5 \times 5$  sampled space points, at each space point's horizontal and vertical HW response  $dx$  and  $dy$  are identified. Here, each sub-region generates 4 dimensional vector by employing HW response and it is given by,

$$v = (\sum dx, \sum dy, \sum |dx|, \sum |dy|) \quad (5)$$

Now, all the sub-regions are concatenated into vectors as  $4 \times (4 \times 4)$ , which results in 64 dimensional vector at each key-points. The following 64 dimensional vectors are employed in performing the matching procedure.

### 3.3 Binary Robust Invariant Scalable Keypoints (BRISK)

BRISK is utilized as a texture descriptor, which attains a significant quality of matching with limited computation time and generate a valuable key-points from an image. Here, it employs a symmetric sampling pattern over sample point of smooth pixels in feature descriptor. The intensity of the image is represented as  $i_x$  and then employ gaussian smoothing with standard deviation  $\sigma_x$ , which is equivalent to the distance between the circle and points.

The key-point  $k$  in an image is patterned according to its scaling and position, the sampling-point pairs are denoted as  $(i_x, i_y)$ . Respectively, the intensity of smoothed values of points is denoted as  $S(i_x, \sigma_x)$  and  $S(i_y, \sigma_y)$ , helps to determine the local gradients. Mathematically, the local gradients  $G(i_x, i_y)$  are represented as follows,

$$G(i_x, i_y) = (i_y - i_x) \cdot \frac{S(i_y, \sigma_y) - S(i_x, \sigma_x)}{\|i_y - i_x\|^2} \quad (6)$$

Assuming, the set  $A$  of sampling point pairs,

$$A = \{(i_x, i_y) \in \mathbb{R}^2 \times \mathbb{R}^2 \mid x < N \wedge y < x \wedge x, y \in \mathbb{N}\} \quad (7)$$

Where,  $N$  is mentioned as the number of sampling point pairs,

Partition the pixel pairs into two sub-sets such as short distance pairs and long distance pairs and it is mentioned as  $d_1$  and  $d_2$  respectively. The following equations represent the distance pairing of sub-sets,

$$\begin{aligned} d_1 &= \{(i_x, i_y) \in A \mid \|i_y - i_x\| < \delta_{\max}\} \subseteq A \\ d_2 &= \{(i_x, i_y) \in A \mid \|i_y - i_x\| < \delta_{\min}\} \subseteq A \end{aligned} \quad (8)$$

Analysis, the local gradient in long distance pairs and not necessary in the global gradient information. The threshold distance is set as  $\delta_{\max} = 9.75t$  and  $\delta_{\min} = 9.75t$  ( $t$  is the scale of  $k$ ). Hence, the point pairs are iterated through  $L$  to identify the complete pattern direction of key points  $k$ , which is given by,

$$G = \begin{pmatrix} G_x \\ G_y \end{pmatrix} = \frac{1}{L} \cdot \sum_{(i_x, i_y) \in L} G(i_x, i_y) \quad (9)$$

Sampling pattern rotation of orientation is mentioned as  $\alpha = \arctan 2(G_y, G_x)$  of the key-point. The binary descriptor  $b_k$  is generated by utilizing short distance paring and each bit in  $b_k$  is calculated from a pair in  $F$ . Hence, the descriptor is

512bits long and it is gathered by performing short distance intensity at every binary feature vectors  $v$ , it is mentioned as follows,

$$v = \begin{cases} 1, & S(i_y^\alpha, \sigma_y) > S(i_x^\alpha, \sigma_x) \\ 0, & \text{otherwise} \end{cases} \quad \forall (i_x^\alpha, i_y^\alpha) \in F \quad (10)$$

Generally, the SIC depends on affine geometrical transform, the following feature combination (SURF and BRISK) provides a better affine geometrical transform. While matching of two satellite images, it contains both inliers and outliers (Inliers represents a correct prediction of features and Outliers represents a wrong prediction of

features). This hybrid feature combination attains a significant rate of inliers.

#### 4. EXPERIMENTAL RESULT AND DISCUSSION

In this section, the experimental results have been characterized in detailed. All experiments were implemented on PC with 1.8GHz Pentium IV processor by employing MATLAB (version 6.5). However, the SIC was illustrated in three different ways, such as standard, with noise and with attack. Here, the two satellite image database of the same scene in different time period was given as the input and it is publicly obtainable database. The sample satellite image database is mentioned and figured as 2,



Figure 2: Input satellite images of the same scene at different time period

##### 4.1 Standard SIC

The following two satellite images were matched by applying BRISK feature. In this feature extraction, the points were detected and matched by computing the pair-wise distance between the feature vectors and it was named as hamming

distance, which is represented in figure 3. Similarly, in SURF feature, the corresponding points were matched by utilizing Sum of Squared Difference (SSD). Matching point using the SURF feature, with the combination of (inliers and outliers) and only with inliers is mentioned in figure 4,



Figure 3: Matching point using BRISK with inliers and outliers, only with inliers

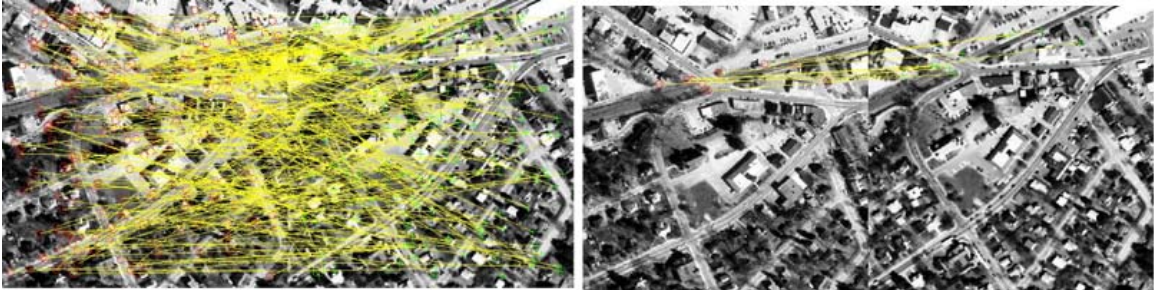


Figure 4. Matching point using SURF with inliers and outliers, only with inliers

Likewise, for the feature combination of BRISK and SURF, the matched points were combined. Matching the point using (BRISK and SURF

feature combination) is specified in figure 5, with the combination of (inliers and outliers) and only with inliers.

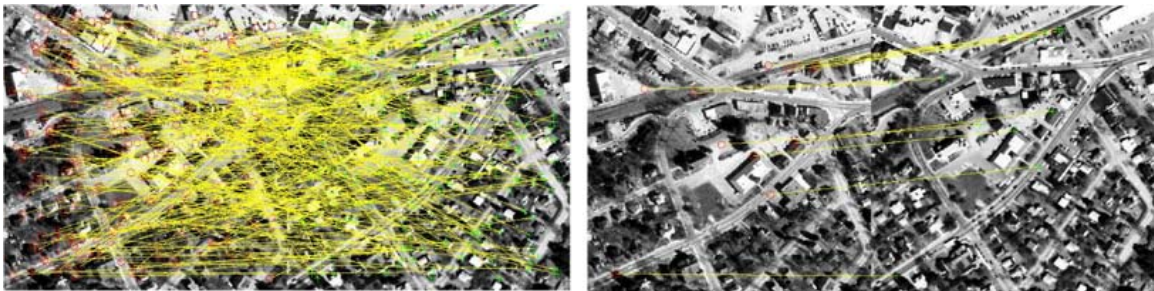


Figure 5: Matching point using BRISK and SURF with inliers and outliers, only with inliers

In this experiment, the quality of SIC is based on affine geometrical transform. While comparing, the geometrical transforms for BRISK and SURF provides a comparable results. But, the combination of BRISK and SURF delivers an effective matching result in co-registration of an image. The final output of BRISK, SURF and the combination of BRISK and SURF is figured as 6, 7, and 8 respectively.



Figure 6: Image registration using BRISK



Figure 8: Image registration using combined BRISK and SURF



Figure 7: Image registration using SURF

#### 4.2 SIC with Noise

Generally, two satellite images are essential to perform SIC. In that, the first image is stationary and the second image is going to register in the first image. Here, SIC with noise demonstrates, including the noise in the second image. Still, the noise factor did not affect the efficiency of repeatability and inliers ratio rate. The final output of SURF and BRISK combination with noise is mentioned in figure 9.



Figure 9: Image registration using combined BRISK and SURF with noise

### 4.3 SIC with Attack

In this section, attack indicates that a particular portion of a satellite image is removed. Similarly, the initial satellite image was kept stationary and the attack factor is applied on second satellite image. Then, the two satellite images were registered, but still it shows a comparable result in repeatability and inliers ratio. The final output of SURF and BRISK combination with an attack is mentioned in figure 10.



Figure 10: Image registration using combined BRISK and SURF with attack

### 4.4 Analysis Report

The accuracy of IR is based on two factors inliers ratio and repeatability. Inliers ratio determines the correct prediction rate of feature matching and repeatability is determined by the mean of the number of detected key-points. Here, the SIC is

demonstrated in three different ways like standard SIC, SIC with noise, SIC with attack. It clearly shows that the combination of SURF and BRISK provides a better registration than other two methods. The performance analysis of features are graphed below in figure 11 and 12 respectively,

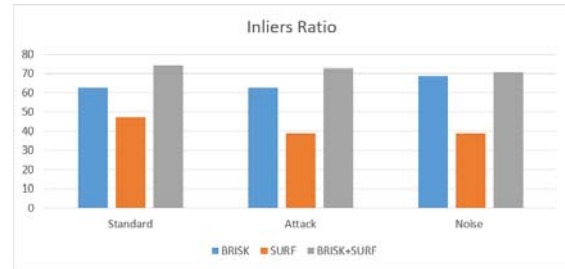


Figure 11: Inliers ratio comparison

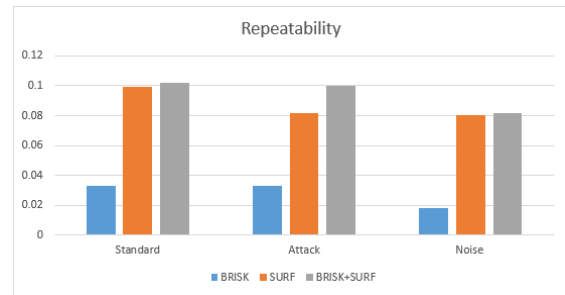


Figure 12: Repeatability comparison

The performance evaluation of following feature combination and the other two methods are evaluated in Table 1. Hence, it proves that the proposed feature combination is very effective in IR, than the other two individual methods.

Table 1: Performance Evaluation of feature combination

Methods	Existing [12]	Proposed scheme								
		Standard			With Noise			With Attack		
		SURF	BRISK	S+B	SURF	BRISK	S+B	SURF	BRISK	S+B
Inliers Ratio	57	47	62.5	74.3	39	68.7	70.4	39	62.5	73
Repeatability	0.09	0.099	0.033	0.102	0.08	0.018	0.0816	0.0814	0.033	0.1

## 5. CONCLUSION

This paper evaluated a hybrid feature combination (SURF + BRISK) for improving the SIC. Usually, the performance of the IR depends on inliers ratio and repeatability. In this scenario, the SIC was illustrated in three different ways, such as standard, with noise and with attack. At standard SIC, the inliers ratio and the repeatability of

proposed combination showed 74.3% and 0.102 values respectively. On the other hand, SIC with noise and SIC with attack showed a superior result in terms of inliers ratio and repeatability, which is significantly greater than the other two individual methods. The outcome of registration was impressive after performing the descriptor level feature combination. In future, the outlier's

rejection rate and inlier's ratio are further improved by employing new intensity based approach in combination with feature based methods.

#### REFERENCES:

- [1] Y. Byun, J. Choi, and Y. Han, "An area-based image fusion scheme for the integration of SAR and optical satellite imagery", *IEEE Journal of Selected Topics in Applied Earth Observations and Remote Sensing*, Vol. 6, No. 5, pp. 2212-2220, 2013.
- [2] Q. Yu, B. Pang, P. Wu, and Y. Zhang, "Automatic coarse-to-precise subpixel multi-band SAR images co-registration based affine SIFT and Radial Base Function (RBF)", *Proceedings of IEEE 5th Asia-Pacific Conference on Synthetic Aperture Radar (APSAR)*, pp. 684-687, 2015
- [3] F. Dell'Acqua, P. Gamba, and G. Lisini, "Coregistration of multiangle fine spatial resolution SAR images", *IEEE Geoscience and Remote Sensing*, Vol.1, No. 4, pp. 237-241, 2004.
- [4] I. De Falco, A. Della Cioppa, D. Maisto, U. Scafuri, and E. Tarantino, "Satellite image registration by distributed differential evolution", *Applications of evolutionary computing*, pp.251-260, 2007.
- [5] Y. Li, and C.H. Davis, "Pixel-based invariant feature extraction and its application to radiometric co-registration for multi-temporal high-resolution satellite imagery", *IEEE Journal of Selected Topics in Applied Earth Observations and Remote Sensing*, Vol. 4., No. 2, pp. 348-360, 2011.
- [6] E.G. Parmehr, C.S. Fraser, C. Zhang, and J. Leach, "Automatic co-registration of satellite imagery and LiDAR data using local Mutual Information", *Proceedings of IEEE International Geoscience and Remote Sensing Symposium (IGARSS)*, pp. 1099-1102, 2013.
- [7] T.A. Teo, and S.H. Huang, "Automatic co-registration of optical satellite images and airborne LiDAR data using relative and absolute orientations," *IEEE Journal of Selected Topics in Applied Earth Observations and Remote Sensing*, Vol. 6, No. 5, pp. 2229-2237, 2013.
- [8] M.I. Patel, V.K. Thakar, and S.K. Shah, "Image Registration of Satellite Images with Varying Illumination Level Using HOG Descriptor Based SURF", *Procedia Computer Science*, pp.382-388, 2016.
- [9] O. Hellwich, C. Wefelscheid, J. Lukaszewicz, R. Hänsch, M.A. Siddique, and A. Stanski, "Integrated matching and geocoding of sar and optical satellite images", *Proceedings of Iberian Conference on Pattern Recognition and Image Analysis*, pp. 798-807, 2013.
- [10] R. Bouchiha, and K. Besbes, "Comparison of local descriptors for automatic remote sensing image registration", *Signal, Image and Video Processing*, Vol. 9, No. 2, pp. 463-469, 2015.
- [11] E.G. Parmehr, C.S. Fraser, and C. Zhang, "Automatic Parameter Selection for Intensity-Based Registration of Imagery to LiDAR Data", *IEEE Transactions on Geoscience and Remote Sensing*, Vol. 54, No. 12, 2016.
- [12] M. Tahoun, A.E.R. Shabayek, R. Reulke, and A.E. Hassanien, "Co-registration of Satellite Images Based on Invariant Local Features", *In Intelligent Systems'*, pp. 653-660, 2015.
- [13] X. Ni, C. Cao, L. Ding, T. Jiang, H. Zhang, H. Jia, G. Li, J. Zhao, W. Chen, W. Ji, and M. Xu, "A fully automatic registration approach based on contour and SIFT for HJ-1 images", *Science China Earth Sciences*, Vol. 55, No. 10, pp. 1679-1687, 2012.
- [14] L.J. Yang, Z. Tian, and W. Zhao, "A new affine invariant feature extraction method for SAR image registration", *International Journal of Remote Sensing*, Vol. 35, No. 20, pp.7219-7229, 2014.
- [15] Y. Ye, and J. Shan, "A local descriptor based registration method for multispectral remote sensing images with non-linear intensity differences", *ISPRS Journal of Photogrammetry and Remote Sensing*, Vol. 90, pp. 83-95, 2014.